Enhancement of the ETS-10 Titanosilicate Activity in the Shape-Selective Photocatalytic Degradation of Large Aromatic Molecules by Controlled Defect Production

ARTICLE *in* JOURNAL OF THE AMERICAN CHEMICAL SOCIETY · MARCH 2003

Impact Factor: 12.11 · DOI: 10.1021/ja027382o · Source: PubMed

J|A|C|S
ARTICLES
Published on Web 01/29/2003

Enhancement of the ETS-10 Titanosilicate Activity in the Shape-Selective Photocatalytic Degradation of Large Aromatic Molecules by Controlled Defect Production

Francesc X. Llabrés i Xamena,[†,‡] Paola Calza,[§] Carlo Lamberti,[†,‡,||] Carmelo Prestipino[†,‡,||] Alessandro Damin,[†,‡] Silvia Bordiga,[†,‡,||] Ezio Pelizzetti,[§] and Adriano Zecchina*[,†,‡]

Contribution from the Dipartimento di Chimica IFM, Università di Torino, Via P. Giuria 7, I-10125 Turin, Italy, INSTM Unitá di Torino Universitá, Turin, Italy, Dipartimento di Chimica Analitica, Università di Torino, Via P. Giuria 5, I-10125 Turin, Italy, and INFM UdR di Torino Università, Turin, Italy

Received June 20, 2002; E-mail: adriano.zecchina@unito.it

Abstract: In recent times, it has been shown that the microporous ETS-10 titanosilicate can be used as a shape-selective photocatalyst for the decomposition of aromatic molecules (*Chem. Commun.* **2001**, 2131). Its actual use on practical grounds is however discouraged by its too low activity, when compared with that of TiO_2 photocatalysts. In the present work, we show how an ad hoc mild treatment with HF enhances the activity of ETS-10 toward the photodegradation of large aromatic molecules that are unable to penetrate inside the zeolitic pores, such as 2,5-dichlorophenol, 2,4,5-trichlorophenol, 1,3,5-trihydroxybenzene, and 2,3-dihydroxynaphthalene (DHN). The photoactivity of the acid-treated materials is comparable or even greater than that of the nonselective TiO_2 catalyst. Moreover, the enhancement of the photoactivity is accompanied by a remarkable parallel increase of the shape selectivity, particularly toward DHN ($k_{DHN}/k_P = 127$, where P = phenol). A complete characterization (by means of X-ray diffraction, scanning electron microscopy, transmission electron microscopy, ultraviolet−visible spectroscopy, and X-ray aborption spectroscopy techniques) of a set of ETS-10 samples which have undergone a progressively severe HF treatment allows us to propose an explanation of the photocatalytic activity and selectivity of the modified materials.

1. Introduction

Heterogeneous photocatalysts based on TiO_2 metal oxides are extensively studied, especially for their application in organic synthesis,[1,2] or in the abatement of hazardous pollutants in water, in air, or on solid surfaces.[3−6] The initiation step of the photocatalytic process consists in the generation of electron−hole pairs upon irradiation of the material with a convenient light source (with an energy greater than its band gap). These photoformed charge carriers can migrate rapidly to the surface of the solid, where they are trapped: electrons produce the reduction of surface Ti(IV) ions into Ti(III), while holes interact (in the presence of water) with formation of •OH and TiO• radical species. These radical species can then initiate the oxidative photodegradation of several organic substrates.

When TiO_2 is used as the photocatalyst, photodegradation processes are nonselective, and thus, the possibility to degrade at will only a given component from a mixture is precluded. Therefore, preparation of selective photocatalysts is an interesting and intriguing goal, as it opens new potential fields of application where nonselective TiO_2 catalysts cannot be used. This can be the case for separation processes, or the selective elimination of (pollutant) molecules from a mixture.

To our best knowledge, only two papers have been published up to now on selective photocatalysts. Ghosh-Mukerji et al.[7] have reported recently the innovative preparation of selective TiO_2 composite photocatalysts, containing specific molecular sites for the recognition of the target molecule in the vicinity of titanium dioxide. Following an alternative approach,[8] we have shown that selective photocatalysis can be obtained through the use of proper molecular sieves (ETS-10) as shape-selective heterogeneous photocatalysts. The activity of the titanosilicate ETS-10[9] has been known for a few years.[8,10,11] This activity is

[†] Dipartimento di Chimica IFM, Università di Torino.
[‡] INSTM Unità di Torino Università.
[§] Dipartimento di Chimica Analitica, Università di Torino.
[||] INFM UdR di Torino Università.

(1) Fox, M. A. *Acc. Chem. Res*. **1983**, *16*, 314−321.
(2) Fox, M. A.; Chen, C. C.; Park, K.; Younathan, N. J. *ACS Symp. Ser*. **1985**, *278*, 69−78.
(3) Fujishima, A.; Honda, K. *Nature* **1972**, *238*, 37−38.
(4) Matthews, R. W. *J. Phys. Chem*. **1987**, *91*, 3328−3333.
(5) Hoffman, M. R. *J. Phys. Chem*. **1987**, *91*, 3328−3333.
(6) Fox, M. A.; Dulay, M. T. *Chem. Rev*. **1993**, *93*, 341−357.
(7) Ghosh-Mukerji, S.; Haick, H.; Schvartzman, M.; Paz, Y. *J. Am. Chem. Soc*. **2001**, *123*, 10776−10777.
(8) Calza, P.; Pazè, C.; Pelizzetti, E.; Zecchina, A. *Chem. Commun*. **2001**, 2130−2131.
(9) Kuznicki, S. M. U.S. Patent 4853202, 1989.
(10) Fox, M. A.; Doan, K. E.; Dulay, M. T. *Res. Chem. Intermed*. **1994**, *20*, 711−722.

10.1021/ja027382o CCC: $25.00

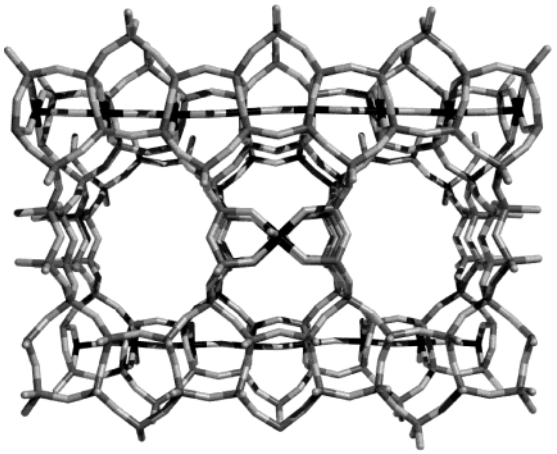

Figure 1. Layout of structural units forming the framework of the titanosilicate ETS-10. Titanium atoms are shown in black, silicon in dark gray, and oxygen in light gray. The extraframework cations (Na^+ and K^+) are not indicated for the sake of clarity.

due to the presence in its structure of photoexcitable Ti−O−Ti chains, and of a three-dimensional interconnected system of large 12-membered SiO_4 ring channels (see Figure 1),[12−14] which endow the material with excellent diffusion properties.[15] This regular channel system (not present in bulk metal oxide semiconductors, such as anatase) has a direct effect in determining the shape selectivity of the degradation process, and this has represented the main achievement of our previous studies on the photodegradation of phenols of different size.[8] In that study, a direct correlation between the size of the molecule and its photodegradability was found: the molecules larger than the diameter of the ETS-10 channels (ca. 0.8 × 0.5 nm) were in fact degraded faster than smaller molecules, for which diffusion at the internal surface of the material was allowed. These results were interpreted in terms of a protective role played by the internal cavities of ETS-10 against the photodegradation of organic molecules (which occurs mainly at the external surface of the crystals). From these results it is clear that, when compared with TiO_2, ETS-10 has the advantage (as commented above) of being a shape-selective photocatalyst. However, its photoactivity is considerably lower, about 1 order of magnitude.[8] Therefore, to render ETS-10 a more attractive material for future applications, improvement of its photocatalytic performance would be highly desired.

To design a strategy, we have taken into account that an increase of surface TiOH groups enhances the photoactivity of TiO_2, having a double effect. On one hand, TiOH groups are effective traps for the photoformed holes, thus reducing their recombination with the electrons. On the other hand, surface OH groups allow the adsorption of O_2[16−18] (usually present in the working medium, i.e., aqueous oxygenated dispersions containing the photocatalyst) and, hence, its reducibility by photoformed electrons. This reduction converts adsorbed O_2 into O_2^- species, which in turn can interact with water with formation of further oxygenated radicals (mainly •OH).[19−22] On this basis, a straightforward way to enhance the photoactivity of ETS-10 could be that of increasing the number of TiOH groups (provided the effect observed in TiO_2 also holds for ETS-10).

In the ideal structure of ETS-10 (see Figure 1), titanium ions are at the center of TiO_6 octahedra, forming linear Ti−O−Ti chains running along two perpendicular directions of the crystal. These octahedra are linked to four SiO_4 tetrahedra through oxygen vertexes. Thus, ETS-10 can be considered as a set of monatomic wires of titanium dioxide embedded into an isolating siliceous matrix.[23−25] In such a structure, titanium centers have their coordination sphere saturated by six oxygen atoms, and consequently, they cannot interact with molecules hosted in the channel system. Following this picture, titanol groups emerge only on the external surfaces, where Ti−O−Ti chains end and hydroxyl groups saturate dangling bonds of titanium ions. However, this material usually presents stacking disorder along the *c* crystallographic axis[12,13] which, together with point defects (produced during the synthesis), can cause breaks in the Ti−O−Ti chains, with subsequent formation of TiOH groups also at internal positions.[26] While the amount of external titanols depends basically on the size and morphology of the crystals, where the TiOTi chains are necessarily interrupted, the concentration of internal titanols reflects the quantity of defects contained in the material. In principle, the amount of internal and external TiOH could be raised by increasing the number of defects contained in the structure and on external surfaces of ETS-10 by means of postsynthesis treatments.

We present here results concerning postsynthesis modifications of ETS-10 via acid treatment with diluted aqueous solutions of hydrofluoric acid. The aim of these (mild) treatments is to increase the amount of accessible Ti sites (titanium centers exposed) without greatly altering the crystallinity of the resulting material. To control possible changes in the crystallinity and in the morphology of the crystals before and after the acid treatments, X-ray diffraction (XRD), scanning electron microscopy (SEM), and high-resolution transmission electron microscopy (HRTEM) have been applied. The effect of treatment with HF on the amount of accessible titanium centers has been evaluated by diffuse-reflectance UV−vis spectroscopy (DRUV−vis), which allows the intensity of the characteristic absorption band of titanium−peroxo complexes formed in the presence of H_2O_2 (which are generated only at accessible titanium sites) to be determined. X-ray absorption spectroscopy (XAFS) has been used on qualitative grounds to evaluate the modification of the

(11) Howe, R. F.; Krisnandi, Y. K. *Chem. Commun*. **2001**, 1588−1589.
(12) Anderson, M. W.; Terasaki, O.; Oshuna, T.; Philippou, A.; Mackay, S. P.; Ferreira, A.; Rocha, J.; Lidin, S. *Nature* **1994**, *367*, 347−351.
(13) Anderson, M. W.; Terasaki, O.; Oshuna, T.; O'Malley, P. J.; Philippou, A.; Mackay, S. P.; Ferreira, A.; Rocha, J.; Lidin, S. *Philos. Mag. B* **1995**, *71*, 813−841.
(14) Rocha, J.; Anderson, M. W. *Eur. J. Inorg. Chem.* **2000**, 801−819.
(15) Kuznicki, S. M.; Thrush, K. A.; Allen, F. M.; Levine, S. M., Hamil, M. M., Hayhurst, D. T.; Mansour, M. In *Molecular Sieves. Synthesis of Microporous Materials*; Occelli, M. L., Robson, H. E., Eds.; Van Nostrand Reinhold: New York, 1992; Vol. I, Chapter 29.
(16) Bickley, R. I.; Stone, F. S. *J. Catal.* **1973**, *31*, 389−397.
(17) Munuera, G.; Rives Arnau, V.; Saucedo, A. *J. Chem. Soc., Faraday Trans. 1* **1979**, *75*, 736−747.
(18) Palmisano, L.; Schiavello, M.; Sclafani, A.; Martra, G.; Borello, E.; Coluccia, S. *Appl. Catal., B* **1994**, *3*, 117−132.
(19) Augugliaro, V.; Palmisano, L.; Sclafani, A.; Minero, C.; Pelizzetti, E. *Toxicol. Environ. Chem*. **1988**, *16*, 89−109.
(20) Okamoto, K.; Yamamoto, Y.; Tanaka, H.; Tanaka, M.; Itaya, A. *Bull. Chem. Soc. Jpn*. **1985**, *58*, 2015−2022.
(21) Okamoto, K.; Yamamoto, Y.; Tanaka, H.; Itaya, A. *Bull. Chem. Soc. Jpn*. **1985**, *58*, 2023.
(22) According to the authors of refs 19−21, reaction of O_2^- with water follows the mechanism $O_2^- + H_2O \rightarrow HO_2^\bullet + {}^-OH$; $HO_2^\bullet + e^- + H_2O \rightarrow H_2O_2 + {}^-OH$; $H_2O_2 + e^- \rightarrow {}^\bullet OH + {}^-OH$.
(23) Borello, E.; Lamberti, C.; Bordiga, S.; Zecchina, A.; Otero Areán, C. *Appl. Phys. Lett.* **1997**, *71*, 2319−2321.
(24) Lamberti, C. *Microporous Mesoporous Mater*. **1999**, *30*, 155−163.
(25) Bordiga, S.; Turnes Palomino, G.; Zecchina, A.; Ranghino, G.; Giamello, E.; Lamberti, C. *J. Chem. Phys.* **2000**, *112*, 3859−3867.
(26) Southon, P. D.; Howe, R. F. *Chem. Mater*. **2002**, *14*, 4209−4218.

Table 1. Most Relevant Properties of the ETS-10 Samples Prepared

sample	HF/H_2O concn (wt %)	relative crystallinity[a] (%)	Ti ← O–O LMCT intensity (Kubelka–Munk)	amt of exposed Ti(IV)[b] (mol of Ti/ g of solid)	amt of exposed Ti(IV) (% Ti total)
ETS-10/0		100	1.4	0.8×10^{-5}	0.5
ETS-10/1	1[c]	98	2.6	1.5×10^{-5}	0.9
ETS-10/2	2[d]	96	3.5	2.1×10^{-5}	1.2
ETS-10/8	8[e]	95	3.9	2.3×10^{-5}	1.3

[a] Determined by XRD. [b] Determined from the curve in Figure 4b. [c] [HF] = 0.56 M. [d] [HF] = 1,13 M. [e] [HF] = 4.52 M.

local environment of Ti species induced by the HF treatment and by interaction with H_2O_2.

To test the photoactivity of the modified ETS-10 samples, two sets of reactions have been investigated: (i) the competitive photodegradation of 4-chlorophenol (CP), 2,5-dichlorophenol (DCP), and 2,4,5-trichlorophenol (TCP) and (ii) competitive photodegradation of phenol (P), 1,3,5-trihydroxybenzene (THB), and 2,3-dihydroxynaphthalene (DHN). The results obtained in each set of experiments using as photocatalyst a commercial TiO_2 sample (Degussa P25) have also been considered for comparison. In both sets of reactions, molecules with different steric hindrance (relative to the diameter of the ETS-10 channels) have been used to check for possible shape-selectivity effects.

2. Experimental Section

The starting (Na,K)-ETS-10 was a commercial sample kindly supplied by Engelhard (Iselin, NJ); its external surface area was 21 m^2 g^{-1} (*t*-plot volumetric measurements with N_2 made with a Micromeritics ASAP 2010 instrument). TiO_2 was a commercial Degussa P25 sample (surface area about 50 m^2 g^{-1}). All the organic compounds (P, CP, DCP, TCP, THB, and DHN) were purchased from Aldrich and used as received.

Acid treatments of the ETS-10 samples were performed with diluted aqueous solutions of HF of different concentrations, ranging form 1% to 8% (wt %). In separate experiments, portions of the solid sample (1.5 g) were contacted with 5 mL of the H_2O/HF solution for a few seconds, then quickly diluted with a large excess of distilled water, filtered under a vacuum, and thoroughly washed with H_2O. These samples will be hereafter denoted ETS-10/*X*, where *X* stands for the concentration (wt %) of HF in the aqueous solution used for the treatment; ETS-10/0 will thus be the untreated (starting) ETS-10 material, which was used here as a reference. In Table 1, the samples prepared and their nomenclature and most relevant properties are reported.

Elemental analysis was performed by measuring the X-ray fluorescence yield of Si, Ti, Na^+, and K^+ on a Philips PW 1404/10 instrument equipped with a double Sc, Mo anode. The Na^+ and K^+ contents were also cross-checked by atomic absorption measurements (ICP-MS instrument equipped with a Perkin-Elmer Elan 5000 mass spectrometer). The amount of H^+ in the HF treated samples was calculated as the difference between the stoichiometry expected value (two monovalemt cations per Ti atom) and the measured Na^+ and K^+ contents. The results obtained showed that the Si/Ti molar ratio progressively decreases from 4.92 (ETS-10/0) to 4.39 (ETS-10/8). These changes are accompanied by a progressive ion exchange of Na^+ (and K^+) by H^+, reaching a maximum fraction, $[H^+]/[Na^+ + K^+ + H^+]$, of 0.45 in the most severely treated sample, Na^+ being the most exchanged cation.

Powder XRD (Cu Kα radiation) of the samples were performed with a Siemens D5000 diffractometer. The high-resolution micrographs were obtained on a JEOL JEM 2000 EX transmission electron microscope equipped with a top entry stage. DRUV−vis spectra were recorded using a Perkin-Elmer Lambda 19 spectrophotometer, in the range 50000−4000 cm^{-1}. The measurements were taken under incipient wetness conditions. XAFS spectra were obtained in the transmission mode, at the EXAFS13 beam line of the DCI storage ring (operating at 1.85 GeV with a typical current of 300 mA) at LURE laboratories in Orsay (France), using air-filled ionization chambers for both incident and transmitted beams. For both detectors the gas pressure has been optimized ad hoc for each sample, maximizing the measured current within the linearity region of the device. The incident beam was monochromatized using a double-crystal Si(111) with a sampling step of 2.0 eV and an integration time of 2.0 s per point. The energy/angle calibration was performed using a Ti foil, and crystals were detuned up to 1/2 of the rocking curve to avoid harmonics. For each sample four equivalent XAFS spectra were acquired under the same experimental conditions and averaged before Fourier filtering.

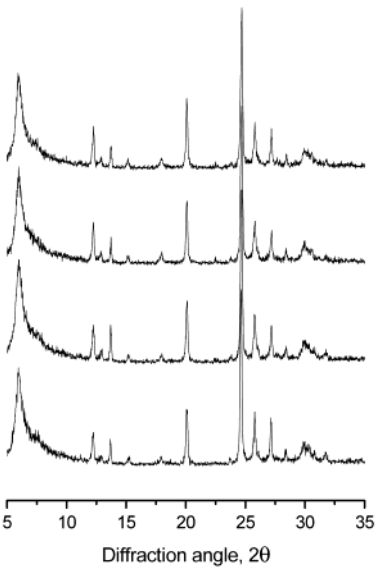

Figure 2. X-ray diffractograms (Cu Kα radiation) of, from bottom to top, ETS-10/0, ETS-10/1, ETS-10/2, and ETS-10/8 samples.

For photocatalytic reactions, the irradiation of the single species was carried out on 5 mL of aqueous suspension containing 1×10^{-4} M organic compound and 1 g dm^{-3} catalyst, using a 1500 W xenon lamp (Solarbox, CO.FO. MEGRA, Milan, Italy) simulating AM1 solar light and equipped with a 310 nm cutoff filter. The total photonic flux in the 310−400 nm range and the temperature in the cell have been kept constant for all the experiments at 1.35×10^{-5} einstein min^{-1} and 323 K, respectively. The disappearance of the primary compound and the intermediate evolution with time were followed using high-performance liquid chromatography (HPLC). A Rheodyne injector, a RP C18 column (Lichrochart, Merck, 12.5 cm × 0.4 cm, 5 μm packing), a high-pressure two-pump gradient (Merck Hitachi L-6200 and L-6000 pumps), and UV−vis detection (Merck Hitachi L-4200) were used. The irradiation of the two equimolar mixtures of the three molecules (i.e., CP/DCP/TCP and P/THB/DHN) was done by using the same conditions as before, and using concentrations of all molecules of 1×10^{-4} M.

3. Results and Discussion

3.1. X-ray Diffraction. X-ray diffraction was used to check the effect of the acid treatments on the crystallinity of the samples prepared as described in the previous section. Figure 2 shows the X-ray diffractograms (Cu Kα radiation) of the acid-modified samples, as well as that of the parent (unmodified) ETS-10 sample. As can be seen from the diffractograms all samples exhibit high crystallinity and are analogous to those reported before.[12,13] No additional peaks belonging to other phases are observed.

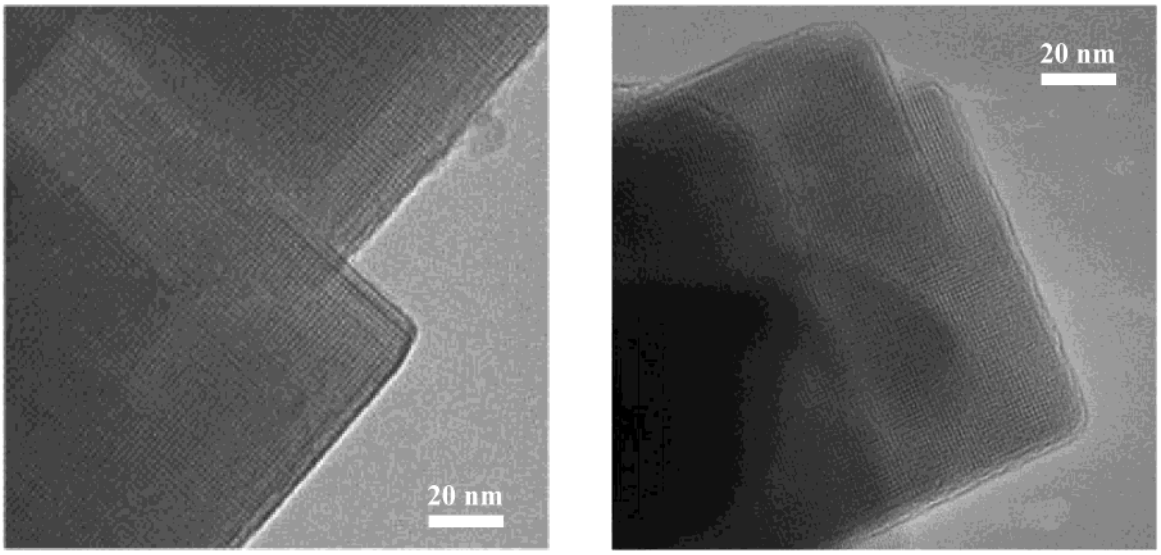

Figure 3. HRTEM micrographs (200 kV, magnification 2×10^5) of the samples ETS-10/0 (left) and ETS-10/8 (right).

The relative crystallinities of the acid-treated samples (Table 1) have been evaluated following standard procedures.[27] The crystallinity of the starting material (ETS-10/0 sample) was arbitrarily assumed to be 100%, and the other values were obtained by considering their relative intensity (peak area) of the diffraction lines near $2\theta = 20°$ and 25°. Silicon (Aldrich, 99.99%) was used as the internal standard. The relative intensities reported in Table 1 are averaged values for several independent measurements of the same sample. According to these values, it can be concluded that in all cases the acid treatment conditions used to modify the ETS-10 samples are mild enough to preserve their crystalline structure. Only a small reduction of the relative crystallinity (less than ca. 5% for the most severely treated sample) of the samples is observed as a consequence of the acid treatment.

3.2. Textural and Morphologic Modification of ETS-10 upon Acid Treatment. The textural characterization of the starting and acid-modified samples was performed by adsorption/desorption isotherms of N_2 at 77 K. The *t*-plot method was used to evaluate the external surface area (S_{ext}). The results obtained show a significant increase of S_{ext} (the associated incertitude being within 2 m^2 g^{-1}), which moves from 21 m^2 g^{-1} for the starting sample up to 27−30 m^2 g^{-1} for the acid-modified samples. The differences observed between the series of acid-treated samples are, however, within the experimental accuracy, and no significant trend among them can be appreciated. No mesopore formation has been observed on HF-treated samples.

Morphologic characterization of ETS-10 samples, prior to and after the acid treatments, was performed by means of SEM and HRTEM. The SEM micrographs obtained are not reported for brevity. The starting material shows cubic-like crystallites ca. 250−300 nm in size. No significant differences are observed as a consequence of the acid treatment: both the morphology and dimensions of the crystallites remain basically unmodified. These results indicate that the modifications produced by the acid treatment occur at a level beyond the detection limit of the SEM, in agreement with the relatively low loss of crystallinity measured by XRD. This means that the induced modifications have nanoscale dimensions (defects).

A better detail of the morphology of the microcrystals can be gained from the HRTEM images shown in Figure 3. The starting ETS-10 sample presents a well-defined pattern of interference fringes. The terminations of the crystals are sharp and well defined, and when terraces are present, they are neat and have well marked steps. After the acid treatment, mild erosion of the crystallite borders is observed, occurring on an atomic scale. The pattern of interference fringes is still well defined, which indicates that the HF treatment has not caused the ETS-10 structure to collapse through the formation of a high concentration of internal defects. This is shown for the case of ETS-10/8, but the same effect was also observed for the other samples.

On the basis of these results, it is concluded that HF mainly corrodes the external surfaces, with appearance of new TiOH groups (vide infra). Finally, it is worth mentioning that, during the HRTEM measurements, a different stability of the ETS-10 samples under the electron beam was observed. In the adopted experimental conditions, the starting ETS-10/0 sample was found to be stable for ca. 1 min of exposure to the electron beam (before the interference fringes start to disappear), while the acid-treated samples started to lose considerably their crystallinity after ca. 30−45 s. This fact can be explained by the differences in the amount of adsorbed water; possibly proton exchange accompanying acid modification results in more strongly adsorbed water in the modified samples that can cause instability under the electron beam.

3.3. DRUV−Vis Spectroscopy: Titration of the Exposed Ti Sites with H_2O_2. It is well-known that exposed Ti(IV) centers (for instance, in TS-1[28]) readily interact with H_2O_2 to give colored yellow-orange surface species absorbing at ca. 26000−28000 cm^{-1}. For this reason, we have used hydrogen peroxide as a titrant molecule of the accessible Ti centers (in the form of exposed TiOH groups) in the ETS-10 samples prepared by acid treatment.

(27) Szostak, R. M. *Zeolites Molecular Sieves*; van Nostrand Reinhold: New York, 1989.

(28) (a) Tozzola, G.; Mantegazza, M. A.; Ranghino, G.; Petrini, G.; Bordiga, S.; Ricchiardi, G.; Lamberti, C.; Zulian, R.; Zecchina, A. *J. Catal.* **1998**, *179*, 64−71. (b) Bordiga, S.; Damin, A.; Bonino, F.; Ricchiardi, G.; Lamberti, C.; Zecchina, A. *Angew. Chem., Int. Ed.* **2002**, *41*, 4734−4737.

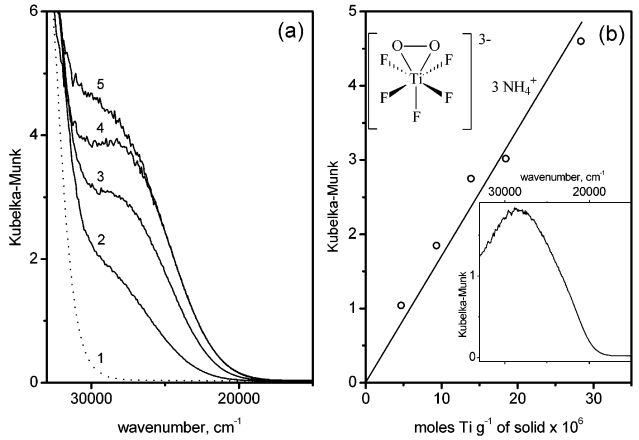

Figure 4. (a) DRUV−vis spectra of the sample ETS-10/0 wetted with pure water (spectrum 1, dotted line) and with an aqueous solution of H_2O_2 (spectrum 2). Spectra 3−5 correspond to the samples ETS-10/1, ETS-10/2, and ETS-10/8 wetted with an aqueous solution of H_2O_2 (same conditions as those of spectrum 2). (b) Calibration curve obtained from solid samples impregnated with aqueous solutions of the coordination complex $(NH_4)_3[Ti(O_2)F_5]$: one of the spectra obtained is shown in the inset. See the text for details.

Figure 4a shows the DRUV−vis spectra obtained for the ETS-10 samples wetted with an aqueous solution of hydrogen peroxide (30% v/v). For comparison, also the spectrum corresponding to the parent ETS-10/0 sample wetted with pure distilled water is presented (spectrum 1, dotted line).

The band at 28000 cm^{-1}, observed for the starting (untreated) ETS-10/0 sample after interaction with H_2O_2 (spectrum 2 in Figure 4a), is attributed to a ligand-to-metal charge-transfer transition (LMCT) of a peroxo-type species formed at exposed titanium sites on the pristine sample. This assignment is confirmed by the fact that a similar band is not present in the spectrum of the ETS-10/0 sample contacted with H_2O (spectrum 1, dotted line).

The LMCT transition band at 28000 cm^{-1} is present with intensification in the spectra of the acid-treated samples (spectra 3−5); i.e., the more severe the acid treatment, the greater the intensity of the LMCT transition band (see Table 1). A neat and progressive increase of its intensity is observed on going from the sample ETS-10/0 (spectrum 2) to ETS-10/2 (spectrum 4). It is therefore clear that, as a consequence of the acid treatment, the quantity of accessible titanium sites is increased as compared to that in the starting material. Since the UV−vis spectra were taken under incipient wetness conditions (H_2O_2 always being in excess), the intensity of the LMCT band is directly related to the concentration of titanium centers exposed.

We notice however that in the sample ETS-10/8 (spectrum 5) only a moderate intensity increase of the LMCT band is observed (from 3.5 to 3.9, Kubelka−Munk), which is accompanied by a blue shift of the maximum, now at 29000 cm^{-1}. These facts seem to indicate that the Ti species present in the sample ETS-10/8 that are able to interact with hydrogen peroxide are somewhat different in nature from those present in the other acid-treated samples. We will see in the following that this fact can have consequences on the photocatalytic performance of the material (section 3.6).

To quantify the amount of titanium centers exposed in the ETS-10 samples, the titanium−peroxo coordination complex $(NH_4)_3[Ti(O_2)F_5]$ was used as a reference to construct a calibration curve (absorbance of the peroxo−titanate vs the concentration of Ti(IV)). To this end, aqueous solutions of $(NH_4)_3[Ti(O_2)F_5]$ of known concentration were prepared and used to impregnate weighed amounts of an inert, white solid having no titanium (silicalite-1). The DRUV−vis spectra of these samples were then recorded in the same conditions adopted for the ETS-10 samples, and the values of the absorbance (Kubelka−Munk) at 28000 cm^{-1} used to construct the calibration curve shown in Figure 4b. The choice of this complex as a reference has some advantages: (i) the complex is soluble in water, thus allowing the simple preparation of reference samples with a known titanium content (expressed as moles of titanium per gram of solid); (ii) the UV−vis spectra of the $(NH_4)_3[Ti(O_2)F_5]$/silicalite-1 samples show an absorption band at 28000 cm^{-1}, which is very similar to that present in the ETS-10 samples upon interaction with H_2O_2. The LMCT bands originating from fluorine ligands occur at much higher frequencies. The most severe limitation associated with the use of $(NH_4)_3[Ti(O_2)F_5]$-impregnated samples as references lies in the assumption that the extinction coefficient of the LMCT transition of the reference compound is essentially identical to that of peroxo species formed on ETS-10 samples upon interaction with H_2O_2. For this reason, the values obtained for the amounts of accessible titanium centers in the ETS-10 samples are considered to be only approximate.

With the limitation discussed above, the acid-treated ETS-10 samples were found to contain an amount of titanium ions which can interact with hydrogen peroxide ranging from ca. 0.5% to 1.3% of the whole structural titanium (the exact value depending on the treatment conditions used; see Table 1). Although the absolute values can be considered as being only approximate, they still represent an estimation of the actual order of magnitude of accessible titanium centers in the acid-modified samples. More reliable information is given by their relative values; i.e., the concentration of Ti(IV) centers that can interact with H_2O_2 is increased about 2.5−3 times on passing from ETS-10/0 to ETS-10/8. The damage of the framework necessary for the formation of such a small concentration of accessible titanium ions at defective positions (involving less than 2% of the whole titanium) prevents the ETS-10 structure from collapsing, as already demonstrated by X-ray diffraction (vide supra).

3.4. XAFS Study. The effect of HF treatments on the local environment of Ti species is shown in Figure 5, where the Fourier transform of the XAFS spectra of the starting sample (dashed curve) and of one of the treated samples (solid curve) are compared. The XAFS spectrum of the as-prepared ETS-10/0 is rather complex and cannot be trivially divided into single first- and second-shell signals, due to the nonequivalence of the Ti−O−Si and Ti−O−Ti bonds and due to the presence of strong multiple scattering contributions caused by the near collinearity of the Ti−O−Ti bonds.[29] This means that any attempt to use this spectrum to derive quantitative results from the EXAFS spectra of the acid-treated ETS-10 samples is precluded. On qualitative grounds we observe a strong modification of the EXAFS signal. The strong reduction of the signal after the acidic treatments is not attributable to a loss of coordination around Ti but to a remarkable heterogeneity of

(29) Sankar G.; Bell, R. G.; Thomas, J. M.; Anderson, M. W.; Wright, P. A.; Rocha J. *J. Phys. Chem.* **1996**, *100*, 449−452.

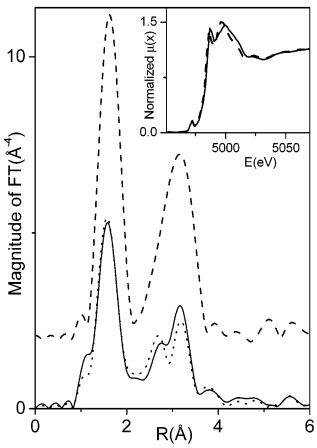

Figure 5. Phase-uncorrected, k^3-weighted Fourier transform of the EXAFS spectra of ETS-10/0 (dashed line), ETS-10/8 (solid line), and ETS-10/8 in interaction with H_2O_2 (dotted line). The inset reports the corresponding near-edge structure for ETS-10/0 (dashed line) and ETS-10/8 (solid line). The XANES spectrum of ETS-10/8 in interaction with H_2O_2 has not been reported, being virtually indistinguishable from that of ETS-10/8.

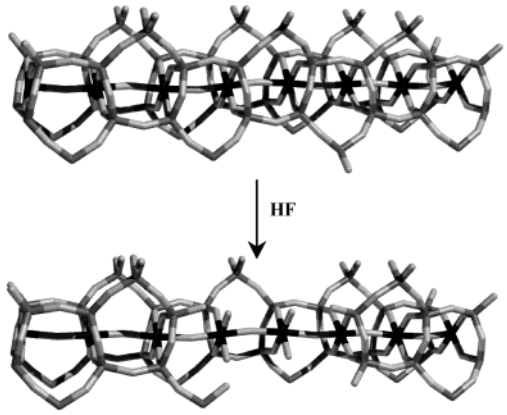

Figure 6. Possible mechanism of defect production on the Ti−O−Ti chains of the ETS-10 titanosilicate during the acid treatment.

the Ti sites generated by HF treatment both directly (elimination of some second-shell Si neighbors) and indirectly (through a partial ion exchange of alkali-metal cations by protons). In fact, it is well-known that the heterogeneity implies a destructive interference among the EXAFS signals of the individual sites, resulting in a damping of the overall signal.[30] On the basis of these qualitative results, it could be inferred that the acid treatment involved a fraction of sites larger than that estimated by the titration method and in contrast with the XRD and HRTEM results. However, XANES spectra (see inset) show that both pre-edge peak and white line intensities are weakly affected by HF treatments, suggesting that the same distorted octahedral geometry of Ti sites holds before and after the acid treatments. This fact agrees with the hypothesis that Ti heterogeneity is the main cause of the reduction of the EXAFS signal. To give an explanation of the high heterogeneity probed by XAFS spectroscopy without invoking the massive creation of defects, we have to take into consideration that partial replacement of Na^+ (and K^+) by H^+ is also taking place as a parallel effect of the acid treatment of ETS-10 with HF solutions (see the elemental analysis in section 2). Moreover, the IR spectra of the acid-treated samples outgassed at 523 K for 30 min (spectra not shown for brevity) show a new IR absorption band centered at 3608 cm^{-1}, which has been assigned[31,32] to the O−H stretching mode of acid-bridged Si(OH)Ti groups. Indeed, upon dosing with NH_3 from the gas phase, formation of NH_4^+ is clearly observed: this is further proof that the ionic exchange by H^+ is occurring during the postsynthesis treatment. The interaction between the negatively charged Ti−O−Ti rows and alkali-metal cations (Na^+ or K^+) is of electrostatic nature, while a significant covalent contribution is expected when protons are present. So this ion exchange is expected to perturb strongly the Ti−O−Ti rows in first-shell Ti−O distances, second-shell Ti−Si and Ti−Ti distances, and especially Ti−O−Si and Ti−O−Ti angles. In this regard, it is worth noting that the imaginary parts of the FT of acid-treated samples with respect to those of the untreated ETS-10/0 sample (not reported for clarity) are not only reduced in intensity but also shifted in phase. This means that a destructive interference occurs between the EXAFS signal generated by unperturbed $[Ti(OSi)_4(OTi)_2](X^+)_2$ units ($X^+ = Na^+$ or K^+) and that generated by the large variety of perturbed units, mainly by ion exchange: $[Ti(OSi)_4(OTi)_2](X^+H^+)$ and $[Ti(OSi)_4(OTi)_2](H^+)_2$. These points fully justify what is observed in Figure 5, without invoking severe framework modifications (elimination of first- and/or second-shell ligands).

Conversely only a few changes have been observed upon interaction of the ETS-10/8 sample with H_2O_2 (compare the solid and dotted line spectra in Figure 5). This evidence reflects the small percentage of Ti species involved in the formation of Ti−peroxo species, in agreement with UV−vis experiments (vide supra section 3.3.).

3.5. Summary of the Characterization Studies. Taking into account the information provided for the above-mentioned techniques (XRD, SEM, HRTEM, DRUV−vis, and XAFS), one can hypothesize that the effect of the acid treatment on the ETS-10 samples consists of the partial solution of the siliceous cover surrounding the Ti−O−Ti chains, in a process analogous to that depicted in Figure 6. This acid attack is mild enough not to alter the crystalline structure. According to the HRTEM micrographs, this attack would affect mainly the external surface of the crystals (which is also consistent with the small contact times used in the preparation of the samples). As a result of the breaking of Ti−O−Si (or Ti−O−Ti) bonds in the subsurface chains, the number of TiOH groups is expected to increase. Moreover, these titanols are not shielded, and thus, they can now interact with molecules adsorbed on the external surface and at the mouth of the channels. Actually, the amount of accessible Ti(IV) sites able to interact with H_2O_2 increases progressively with the concentration of HF in the solution used for the preparation of the sample, as stated by DRUV−vis spectroscopy. The model reported in Figure 6 is also able to explain the changes observed in the EXAFS data of the acid-treated ETS-10 samples after interaction with H_2O_2: in fact the formation of a single Ti−peroxo complex in the exposed part of the Ti−O−Ti chain will perturb not only the involved Ti atom but also those adjacent to it.

(30) Lamberti, C.; Bordiga, S.; Zecchina, A.; Salvalaggio, M.; Geobaldo F.; Otero Areán, C. *J. Chem. Soc., Faraday Trans.* **1998**, *94*, 1519−1525.
(31) Zecchina, A.; Llabrés i Xamena, F. X.; Pazè, C.; Turnes Palomino, G.; Bordiga, S.; Otero Areán, C. *Phys. Chem. Chem. Phys.* **2001**, *3*, 1228−1231.
(32) Zecchina, A.; Pazè, C.; Otero Areán, C.; Turnes Palomino, G.; Llabrés i Xamena, F. X.; Bordiga, S. *Stud. Surf. Sci. Catal.* **2001**, *135*, 274−274.

Table 2. Photodegradation Rates for an Equimolar Mixture of CP, DCP, and TCP[a]

	rate ($M \times 10^5$ min^{-1})		
	TiO_2	ETS-10/0	ETS-10/2
CP	2.87 (1)	0.14 (1)	0.15 (1)
DCP	2.78 (0.97)	0.20 (1.43)	1.03 (7.05)
TCP	2.71 (0.94)	0.54 (3.86)	1.69 (11.6)

[a] The values in parentheses are the relative degradation rates of DCP and TCP with respect to CP over a given catalyst.

Table 3. Photodegradation Rates for an Equimolar Mixture of P, THB, and DHN[a]

	rate ($M \times 10^5$ min^{-1})			
	TiO_2	ETS-10/0	ETS-10/2	direct photolysis
P	2.77 (1)	0.08 (1)	0.08 (1)	ND
THB	5.74 (2.07)	0.38 (4.75)	4.30 (54)	ND
DHN	7.90 (2.85)	4.46 (55.7)	10.20 (127)	0.21

[a] The values in parentheses are the relative degradation rates of THB and DHN with respect to P over a given catalyst. The values determined for the direct photolysis of the products are also presented in the rightmost column.

3.6. Photocatalytic Activity of the Samples. One of the aims of the present study is to compare the photocatalytic activity of the acid-treated ETS-10 with that of the well-known TiO_2 (Degussa P25), i.e., the natural reference for all photodegradation catalysts.

To test the selective photoactivity of ETS-10, molecules of different steric hindrance were degraded; (poly)chlorinated and (poly)hydroxylated aromatic compounds have been chosen. The study of the photodegradation of phenol and chlorophenols presents two main advantages: (i) they have already been studied on TiO_2,[34] and (ii) in the case of chlorophenols, the parallel determination of the disappearance rate and of the chloride evolution provides a good confirmation of the effective degradation of the molecules.

The activity of untreated ETS-10 in the photocatalytic degradation of organic molecules and its selectivity toward large aromatic molecules have already been proved.[8] The activity and selectivity of ETS-10 increase progressively with increasing HF treatment, reaching a maximum for the sample ETS-10/2 and then slightly decreasing. These results indicate, as already suggested by the DRUV−vis study (vide supra section 3.3), that the HF treatment on sample ETS-10/8 has gone slightly beyond the optimal limit. Because ETS-10/2 is the most interesting sample, the discussion in subsections 3.6.1 and 3.6.2 will be focused on it.

3.6.1. Competitive Photodegradation of (Poly)chlorinated Aromatic Compounds. A set of three chlorophenols, characterized by increasing steric hindrance (i.e., CP, DCP, and TCP), was tested. The results of the photodegradation experiments are reported in Table 2. In the same table the results obtained by using TiO_2 as a photocatalyst in the same experimental conditions are reported for comparison. For all tested molecules ETS-10/0 shows a photocatalytic activity that is generally more than 1 order of magnitude lower than that of TiO_2, while as far as ETS-10/2 is concerned this holds only for CP, the activity toward DCP and TCP being comparable to that of TiO_2.

Adopting TiO_2 as photocatalyst, CP, DCP, and TCP show the same rate of disappearance, while by employing ETS-10/0 a selective degradation is observed; TCP is degraded with a rate constant ratio of 3.86 (i.e., k_{TCP}/k_{CP}, values in Table 2). A more interesting selectivity is shown when ETS-10/2 is adopted. With this material, the rate of disappearance of chlorophenol remains the same as that in the virgin sample (0.15×10^{-5} M min^{-1}), while that of DCP increases ($k_{DCP}/k_{CP} = 7.05$), and a further increase is observed with TCP ($k_{TCP}/k_{CP} = 11.6$). These results suggest that, like in TiO_2, the photocatalytic active sites of ETS-10 samples are titanols linked on external surfaces where the −Ti−O−Ti−O−Ti− chains emerge and the Ti−O−Si (or Ti−O−Ti) bonds are consequently broken (vide supra section 3.5). The acidic treatment has increased the availability of titanols in the external surface, and this leads to an increased rate of disappearance for the molecules that react at the external surface of the material (DCP and TCP).

The bulk Ti atoms of ETS-10 cannot be considered as playing a role in the degradation for two reasons: (i) we have demonstrated that Ti species located in perfect Ti−O−Ti rows are not active;[8] (ii) as far as defective sites are concerned, it has been shown[35,36] that when degradation takes place at centers located in restricted spaces (such as titanols in defects located inside the zeolitic channels), the intermediate degradation products are able to back-react with active species, favoring recombination. Furthermore, due to the extinction phenomenon, it is evident that the number of UV photons reaching the internal Ti sites is lower than at the surface of the solid. It is a matter of fact that chlorophenol, which can easily diffuse inside the cavities because of its reduced size, is preserved from the degradation in both cases (ETS-10/0 and ETS-10/2). This explains why its degradation occurs in both cases with the same (very low) rate.

3.6.2. Competitive Photodegradation of (Poly)hydroxylated Aromatic Compounds. The photodegradation of hydroxylated aromatic compounds was also studied; in this case, the size of the molecules increases on going from P to THB and to DHN.

These molecules show an interesting selectivity. This is particularly evident by comparing P and DHN degradation, DHN being degraded on ETS-10/0 with a rate which is 55.7 times higher than that of P (and 4.75 times higher in the case of THB) and with a degradation efficiency on the same order as that of TiO_2 (data reported in Table 3). With TiO_2 the rate is similar for the three species. In the same conditions the contribution of direct photolysis is negligible. Adopting ETS-10/2, the rate of P remains equal (same considerations as above) while the rate increases markedly for THB ($k_{THB}/k_P = 54$) and for DHN ($k_{DHN}/k_P = 127$). In this last case the rate becomes ever higher than for TiO_2; this material has overcome the limit linked to the use of ETS-10 as an effective photocatalyst.

In a mixture containing P, THB, and DHN, by irradiation with ETS-10/2, we can obtain the complete abatement of DHN in 10 min (see Figure 7), while the phenol concentration is basically unmodified. By irradiating for 20 min, THB is also completely degraded, while phenol is still preserved from degradation (only 10% disappears).

(33) Minero, C.; Pelizzetti, E.; Malato, S.; Blanco, J. *Chemosphere* **1993**, *26*, 2103−2119.
(34) Serpone, N.; Sauvé, G.; Koch, R.; Tahiri, H.; Pichat, P.; Piccinini, P.; Pelizzetti, E.; Hidaka, H. *J. Photochem. Photobiol., A* **1996**, *94*, 191−203.
(35) Minero, C. *Catal. Today* **1999**, *54*, 205−216.
(36) Cunningham, J.; Al-Sayyed, G.; Sedlak, P.; Caffrey, J. *Catal. Today* **1999**, *53*, 145−158.

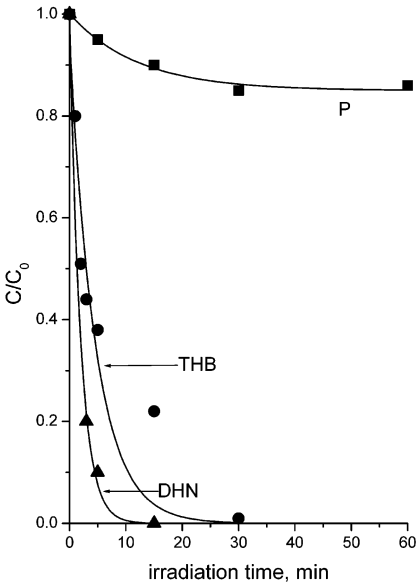

Figure 7. Photodegradation curves of the three hydroxylated aromatic compounds over the acid-treated ETS-10/2 sample as a function of time.

In view of the results obtained and of the fact that catalytic centers are located on the external surface, it can be concluded that the zeolitic internal cavities offer a protective environment against degradation to those species that, because of their small size, can easily diffuse inside. A further confirmation of the presence of catalytic sites on the external surface is given by the fact that the degradation rate of DHN on TiO_2 and on ETS-10, which have similar external surface areas, is of the same order of magnitude. The shielding effect of ETS-10 against photodegradation is particularly marked for P, which is the smallest molecule investigated, and not present for DHN, which is the only studied species whose size surely does not fit the channel size, and so it is the most degraded molecule. The ability to diffuse inside the cavities seems then the main factor determining the shape-selective degradation. However, it is worth noting that even if the previous hypothesis appears as the simplest way to explain the observed shape selectivity of ETS-10, a "pore-mouth" selectivity cannot be a priori excluded as a contributing mechanism. In fact, as photodegradation of the organic molecules takes place at the external surface of the crystals, the ability of the organic species to accommodate in the vicinity of the pore mouth (where the Ti−O−Ti chains end) could also be important in determining its degradation rate. In this case, the mechanism of the selectivity would be different from that proposed above (in which the differences in the photodegradability are attributed only to differences in the ability to diffuse inside the channel system). Whatever the contribution of the two mechanisms, it is important to stress that in both cases we are dealing with shape selectivity.

4. Conclusions

Mild postsynthesis treatments of ETS-10 molecular sieves with diluted HF/H_2O solutions are found to be a convenient method to enhance surface reactivity, as compared to that of the as-synthesized material. Mild conditions (diluted acid solutions and short contact times) have to be adopted to prevent the crystal structure of the solid from collapsing. The resulting materials show an amount of accessible titanium sites (most likely in the form of titanol groups) which is up to 2.5−3 times larger than in the parent material. Partial solution of the siliceous cover surrounding the Ti−O−Ti chains in the ETS-10 structure, with consequent breaks of Ti−O−Si (or Ti−O−Ti) linkages, seems the most likely origin of these accessible titanium sites.

The acid-treated ETS-10 samples present an enhanced activity in the photodegradation of organic molecules as compared to that of the parent ETS-10: polychlorinated and polyhydroxylated aromatic compounds have been considered here as reaction tests. More important, the increase of activity in acid-modified samples is also accompanied by a greater morphoselectivity.

Acknowledgment. The present work is a part of a project coordinated by A. Zecchina and co-financed by the Italian MURST (Cofin 2000, Area 03). We thank R. Buzzoni and L. Grande (Polimeri Europa SpA, Istituto "G. Donegani", Novara) for the elemental analysis, and G. Spoto for the HRTEM investigation. The Secretaría de Estado de Educación y Universidades of Spain is also gratefully acknowledged for a postdoctoral grant to F.X.L.i.X. The constructive comments/suggestions of the reviewers are acknowledged.

JA027382O